A summertime rainy season in the Arctic forests of the Eocene

Brian A. Schubert[1]*, A. Hope Jahren[1], Jaelyn J. Eberle[2], Leonel S.L. Sternberg[3], and David A. Eberth[4]
[1]Department of Geology and Geophysics, University of Hawaii, Honolulu, Hawaii 96822, USA
[2]University of Colorado Museum of Natural History and Department of Geological Sciences, University of Colorado, Boulder, Colorado 80309, USA
[3]Department of Biology, University of Miami, Coral Gables, Florida 33124, USA
[4]Royal Tyrrell Museum of Palaeontology, Drumheller, Alberta T0J 0Y0, Canada

ABSTRACT

The discovery of exceptionally well-preserved fossil wood revealed that extensive forests existed north of the Arctic Circle during the Eocene (ca. 45–55 Ma). Subsequent paleobotanical studies led researchers to suggest eastern Asia as a modern analog, based on the distribution of nearest living relatives. During the last decade, proxy-based reconstructions of mean annual paleoprecipitation, productivity, and relative humidity have led workers to characterize the climate of the Arctic forests as similar to today's temperate forests of the Pacific Northwest. Using a new model, we reconstructed the seasonal timing of paleoprecipitation from high-resolution intra-ring carbon isotope measurements of fossil wood. We showed that the Eocene Arctic forests experienced, on average, 3.1 times more precipitation during summer than winter, entirely dissimilar to the Pacific Northwest where summer precipitation is only one-half to one-sixth of the winter precipitation. This new result shows that although mean annual climate conditions may have been similar to the mean annual conditions the Pacific Northwest, consideration of seasonality implies that the temperate forests of eastern Asia represent the best overall modern analog for the Eocene Arctic forests.

INTRODUCTION

Buried within the permafrost of the Canadian High Arctic are the fossilized remains of vast conifer forests that thrived for millions of years during the Eocene epoch. These northern high-latitude areas supported species-rich plant (Jahren, 2007; McIver and Basinger, 1999) and vertebrate (Eberle et al., 2009; Eberle and McKenna, 2002; Estes and Hutchison, 1980) communities that endured at least three months of nearly continuous (>22 h/d) light and dark periods each year (Herman and Spicer, 2010). Although mild winter temperatures suggest that these Eocene Arctic paleoenvironments were likely free of permafrost (Basinger et al., 1994; Eberle et al., 2010; Estes and Hutchison, 1980; Greenwood et al., 2010; Markwick, 1998), photosynthesis ceased during the dark polar winter. Similar ecosystems do not exist at these latitudes today, but comparison of the nearest living relatives to the flora and fauna of the Eocene Arctic led researchers to propose parts of eastern Asia as a modern analog to the Arctic Eocene forests (Basinger, 1991; Basinger et al., 1994; Estes and Hutchison, 1980; Kalgutkar and McIntyre, 1991; McIntyre, 1991; McIver and Basinger, 1999). More recent work has used paleoreconstructions of the climate, biomass, and productivity of the fossil forests to infer a modern analog climate environment. Specifically, estimates of mean annual precipitation (MAP) (Greenwood et al., 2010), paleotemperature and relative humidity (Jahren and Sternberg, 2003), and biomass and productivity (Williams et al., 2003) led these researchers to compare the Arctic Eocene conifer forest environment to the present-day Pacific Northwest. For example, Vancouver Island, British Columbia, has a MAP of 1452 mm and a mean annual temperature (MAT) of 8.6 °C (Greenwood et al., 2010), values that fall within the ranges estimated for the Eocene Arctic from plant and animal fossils (Table 1). Both eastern Asia and the Pacific Northwest have similar MAT and MAP, but differ critically in the seasonal

timing of maximum precipitation. In the Pacific Northwest, the amount of summer precipitation represents one-half to one-sixth the amount of winter precipitation, which is in stark contrast to eastern Asia where two to six times more precipitation falls in summer than winter. Here we report high-resolution (intra-ring) carbon isotope measurements across fossil tree rings in order to provide the first quantitative estimates for the seasonal distribution of precipitation in the Arctic during the Eocene.

MATERIALS AND METHODS

Five mummified (i.e., nonpermineralized), fossil wood samples collected from deltaic deposits from two geographically distant sites—the Margaret Formation at Stenkul Fiord on southern Ellesmere Island, Nunavut, and the Cyclic Member of the Eureka Sound Formation on northern Banks Island, Northwest Territories—were sampled for high-resolution, intra-ring $\delta^{13}C$ analyses (G13, A15A16, MB, CMNPB4720, and CMNPB4723; Fig. DR1 in the GSA Data Repository[1]). Both sites were located at ~76°N during the Middle to Early Eocene, but were separated by ~40° of longitude (~1100 km) (GEOMAR, 2011; Irving and Wynne, 1991). We estimated seasonal precipitation for the Eocene Arctic on the basis of 812 $\delta^{13}C$ measurements across 20 tree rings from the five fossils (Table 2; Fig. 1). The number of trees, growth rings, subsamples, and measurements per ring we analyzed here exceeded the median numbers analyzed in 11 previous studies of modern trees (n = 2 trees, n = 16 growth rings, n = 84 subsamples, n = 9 measurements per ring; calculated from Table 2 within Schubert and Jahren, 2011). Each sample was subdivided

TABLE 1. COMPARISON OF THE TEMPERATURE (°C), PRECIPITATION (mm), AND SUMMER RELATIVE HUMIDITY (%) OF MODERN BRITISH COLUMBIA AND SOUTH KOREA TO THAT OF THE ARCTIC EOCENE

	Campbell River, BC*	Busan, South Korea[†]	Gangneung, South Korea[†]	Arctic Eocene[§]
MAT	8.6	14.4	13.4	8–15
CMMT	1.3	3.0	1.3	−2–5.5
WMMT	16.9	25.7	24.5	19–25
MAP	1452	1548	1645	1500
P_{summer}	429	1171	1253	1134
P_{winter}	1023	377	392	366
P_{summer}/P_{winter}	0.4	3.1	3.2	3.1
RH_{summer}	58–74	65–85[#]	61–79[#]	67–100**

Note: BC—British Columbia; MAT—mean annual temperature; CMMT—cold month mean temperature; WMMT—warm month mean temperature; MAP—mean annual precipitation; P_{summer}—May through October precipitation; P_{winter}—November through April precipitation; RH_{summer}—May through October relative humidity.
*As reported in Environment Canada (2011).
[†]As reported in NOAA Climate Services (2011).
[§]Temperature estimates summarized in Eberle et al. (2010) and Jahren and Sternberg (2003); MAP from Greenwood et al. (2010).
[#]As reported in Korea Meteorological Administration (2011).
**Jahren and Sternberg (2003, 2008).

*E-mail: bschube@hawaii.edu.

TABLE 2. SUMMARY OF EVERGREEN WOOD SAMPLES ANALYZED

Sample ID	Median resolution (µm)	Avg. no. $\delta^{13}C$ analyses per ring	$\Delta\delta^{13}C_{meas}$ (‰)	P_1/P_2*
Ellesmere Island				
G13	30	66	0.46	4.1
A15A16	40	67	0.99	2.2
MB	63	21	0.54	3.7
Banks Island				
CMNPB4720	78	30	0.76	2.9
CMNPB4723	50	20	0.77	2.8
Average	52	41	0.70 ± 0.21	3.1

*Ratio of summer (P_1) to winter (P_2) precipitation, calculated using Equation 1 of the text.

by hand using a razor blade into 30–78 µm increments (Table 2) to determine bulk $\delta^{13}C$ values across each tree ring (see the Data Repository). The number of $\delta^{13}C$ measurements per ring measured here (n = 41) represents significantly higher resolution than our previous work on Eocene fossil wood (n = 9; Jahren and Sternberg, 2008). Three out of five fossils showed distinctive, concentric rings in hand sample (Figs. DR1C–DR1E), so the direction of growth was known; tree rings were not observed in G13 and A15A16 due to taphonomic processes (Figs. DR1A and DR1B). All of the samples were from different stratigraphic layers (Figs. DR2–DR4), and consequently rings of different samples were not correlated.

We determined the fossil wood samples from Stenkul Fiord to be Early Eocene in age (ca. 53–54.5 Ma) based primarily upon the composition of the vertebrate fauna that includes mammals and several taxa of turtle, and to a lesser extent a preliminary radiometric date; fossil wood from Banks Island was determined to be Eocene in age based upon the palynology and fossil vertebrates (see the Data Repository).

RESULTS AND DISCUSSION

In order to quantify seasonal precipitation across the Canadian Arctic, we conducted high-resolution carbon isotope analyses on five wood samples (Fig. DR1). Across three samples with preserved ring anatomy, the lowest $\delta^{13}C$ values corresponded with the ring boundaries and the highest $\delta^{13}C$ values occurred in the middle of the growing season (Figs. 1C–1E). Ring boundaries were inferred for the other two fossils based on similarities in the $\delta^{13}C$ pattern among all five samples (Fig. 1). High-resolution $\delta^{13}C$ measurements across wood can be used to infer annual growth ring boundaries in modern species (Leavitt and Long, 1991), including wood that lacks identifiable ring anatomy (e.g., Pons and Helle, 2011). The $\delta^{13}C$ pattern does not differ between angiosperm and gymnosperm trees, but does differ strongly between evergreen and deciduous trees. The $\delta^{13}C$ patterns, with mid-season maxima in $\delta^{13}C$ values for all fossils (Fig. 1), indicate an evergreen habit (Barbour et al., 2002), and are in strong contrast to the steady decrease in $\delta^{13}C$ values observed in modern (Helle and Schleser, 2004) and ancient (Jahren and Sternberg, 2008) deciduous trees (see the Data Repository).

The resulting $\delta^{13}C$ trends of fossil angiosperm or gymnosperm evergreen wood can be used to calculate the ratio of summer to winter precipitation (P_1/P_2) across the Eocene Arctic using the following relationship derived from Equation 9 of Schubert and Jahren (2011) (see the Data Repository):

$$\ln\left(P_1/P_2\right) = \left(\Delta\delta^{13}C_{meas} - \Delta\delta^{13}C_{CO_2} - 0.73\right) / (-0.82), \quad (1)$$

where $\Delta\delta^{13}C_{CO_2} = 0.01L + 0.13$ (L = latitude, valid only for Northern Hemisphere sites), and $\Delta\delta^{13}C_{meas}$ is the average difference between the maximum $\delta^{13}C$ value of a given year ($\delta^{13}C_{max}$) and the preceding minimum
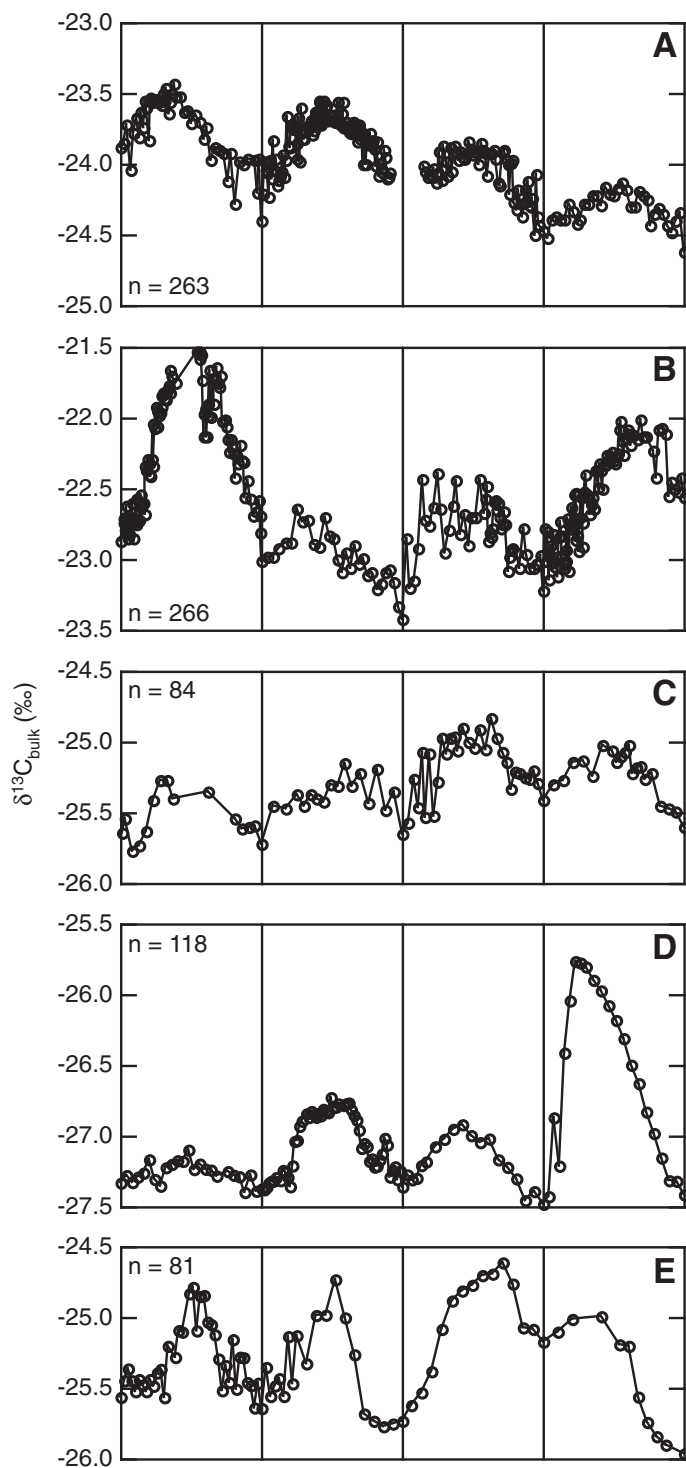

Figure 1. High-resolution $\delta^{13}C$ measurements across nonpermineralized, fossil wood. The $\delta^{13}C$ patterns from five different Eocene wood pieces recovered from Ellesmere Island (A, G13; B, A15A16; C, MB) and Banks Island (D, CMNPB4720; E, CMNPB4723) indicate trees were evergreen. Average $\Delta\delta^{13}C_{meas}$ of the evergreen trees for all sites was equal to 0.70‰ (0.66‰, Ellesmere Island; 0.76‰, Banks Island). Ring boundaries (vertical lines) in A and B were inferred from the isotopic pattern; rings boundaries in C–E were identified from wood anatomy and confirmed by the isotopic pattern. The direction of growth is from left to right for C–E; growth direction is unknown for A and B.

$\delta^{13}C$ value of the annual cycle ($\delta^{13}C_{min}$). Equation 1 results from a comparison of high-resolution $\delta^{13}C$ data on 286 annual growth rings in modern evergreen trees to a suite of environmental characteristics at the site of growth. The trees included in this relationship represent ten different evergreen genera, including both angiosperms and gymnosperms, growing across 98° of latitude and all temperature and precipitation regimes in which evergreen trees are able to grow. The data set includes high-latitude locations, near the tree line, with large changes in seasonal light levels (e.g., northern Sweden, 64°N; central Siberia, 60°N), and places where tree growth ceases in winter due to subfreezing temperatures (e.g., Italian Alps, Sweden, Siberia, and Germany). Across all sites, we had very high correlation ($R^2 = 0.96$) between the measured and predicted change in $\delta^{13}C$ (see Schubert and Jahren, 2011, their equation 9 and figure 7).

The average $\Delta\delta^{13}C_{meas}$ value calculated from carbon isotope measurements on five Eocene evergreen trees sampled from across the Canadian Arctic (Fig. 1) is 0.70‰ with a standard deviation of 0.21‰ (Table 2). Given that $L = 76$ (GEOMAR, 2011; Irving and Wynne, 1991) and $\Delta\delta^{13}C_{meas} = 0.70‰ \pm 0.21‰$ for these sites during the Eocene, Equation 1 revealed $P_1/P_2 = 3.1$ (i.e., 2.4 to 4.0), or 3.1 times more precipitation in summer than winter (Table 2). This calculation assumed that, for Northern Hemisphere sites, seasonal changes in $\delta^{13}C_{CO_2}$ ($\Delta\delta^{13}C_{CO_2}$), which are reflected in the $\delta^{13}C$ values measured in bulk wood, were of the same magnitude and followed the same latitudinal trends as today ($\Delta\delta^{13}C_{CO_2} = 0.01L + 0.13$; Keeling et al., 2001; Schubert and Jahren, 2011). Warm winter conditions over midlatitudes, however, may have resulted in a dampening of the seasonal $\delta^{13}C_{CO_2}$ signal. A decrease in $\Delta\delta^{13}C_{CO_2}$ of up to 40% compared to modern values still results in $P_1/P_2 > 2$ (at least twice as much summer precipitation as winter precipitation). In contrast, increased photosynthesis at high latitudes might imply that the latitudinal trend in $\Delta\delta^{13}C_{CO_2}$ during the Eocene was steeper than today; this scenario serves to increase P_1/P_2 and implies that an even larger proportion of the annual precipitation fell during summer. Likewise, although seasonal changes in light levels proved insignificant in our model, sites in our model only extended up to 64°N (Schubert and Jahren, 2011). Above the Arctic Circle it is possible that the extreme photoperiod could more strongly influence the $\delta^{13}C$ pattern. On the basis of isotope theory, these changes in seasonal light would serve to increase $\Delta\delta^{13}C_{meas}$, which would result in an increase in our estimate for P_1/P_2. Lastly, taking error into account for the estimate of paleolatitude from Irving and Wynne (1991), the fossil forest sites may have been as far south as 74°N, which would only decrease our estimate of P_1/P_2 by 0.1 ($P_1/P_2 = 3.0$ versus 3.1); higher paleolatitudes would serve to increase P_1/P_2. Therefore, taking all the above uncertainties into account, our estimate for P_1/P_2 may represent a minimum value. $\Delta\delta^{13}C_{meas}$ values differ slightly for each evergreen wood sample ($\Delta\delta^{13}C_{meas} = 0.46‰–0.99‰$) (Table 2), but were not significantly different between Ellesmere Island ($\Delta\delta^{13}C_{meas} = 0.66‰ \pm 0.28‰$, n = 3) and northern Banks Island ($\Delta\delta^{13}C_{meas} = 0.76‰ \pm 0.009‰$, n = 2). The similarities between the data from Ellesmere Island and Banks Island suggest that wet summers characterized the regional Arctic climate during the Eocene. The range in $\Delta\delta^{13}C_{meas}$ values for each fossil yielded P_1/P_2 values between 2.2 and 4.1 (Table 2), indicating these trees grew under conditions with approximately two to four times greater precipitation in summer than in winter. When taken with independent estimates of MAP, values for summer and winter precipitation can be quantified. MAP for Late Paleocene (Ellesmere Island, 1000–2190 mm/yr) and Middle Eocene (Axel Heiberg Island, 930–1900 mm/yr) sites was estimated using leaf-area analysis and bioclimatic analysis based upon nearest living relatives (Greenwood et al., 2010). If we use the midpoint value within the large range of MAP given above, 1500 mm ($P_1 + P_2 = 1500$ mm), and our average value for P_1/P_2 is 3.1, we calculate $P_1 = 1134$ mm (mean summer precipitation) and $P_2 = 366$ mm (mean winter precipitation).

Examination of our seasonal precipitation estimates revealed that the moisture regime across the Eocene Arctic was similar to that of present-day eastern Asia (MAP = 1000–2000 mm; $P_1/P_2 = 1.3–5.8$), but not to that of the Pacific Northwest (MAP = 1000–2000 mm; $P_1/P_2 = 0.16–0.53$), where summers receive as little as one-sixth the precipitation as in winter (Fig. 2). Annual and seasonal temperatures and relative humidity for eastern Asia are also similar to those estimated for Arctic Canada during the Eocene (Table 1). Model results indicate high humidity and cloudiness in winter (Abbot et al., 2009), although precipitation or summertime cloudiness was not modeled. Our data indicating abundant precipitation during the summer suggest a high amount of summer water vapor, which is consistent with proxy-based estimates of high amounts of atmospheric water and increasing relative humidity during the growing season (Jahren and Sternberg, 2003, 2008). If the relationship between humidity and cloudiness modeled by Abbot et al. (2009) for winter months also applies to summer months, we can speculate that summers may have had greater cloudiness than winters. With our new insight into the seasonal precipitation regime in the Arctic during the Eocene, we conclude that both paleobotanical and paleoenvironmental evidence are consistent with eastern Asia as the best modern analog for the Arctic Eocene forests (Table 1; Fig. 2).

Above the Arctic Circle, the extreme photoperiod limits photosynthesis to the summer season. Freshwater availability during summer months was required to support photosynthetic organisms in both terrestrial and marine realms. Thus, seasonal precipitation focused in summer months made possible the existence of forests north of the Arctic Circle and could possibly have contributed to the vast *Azolla* communities of the Arctic Ocean (Barke et al., 2011; Brinkhuis et al., 2006; Greenwood et al., 2010), which require freshwater (and light) to bloom.
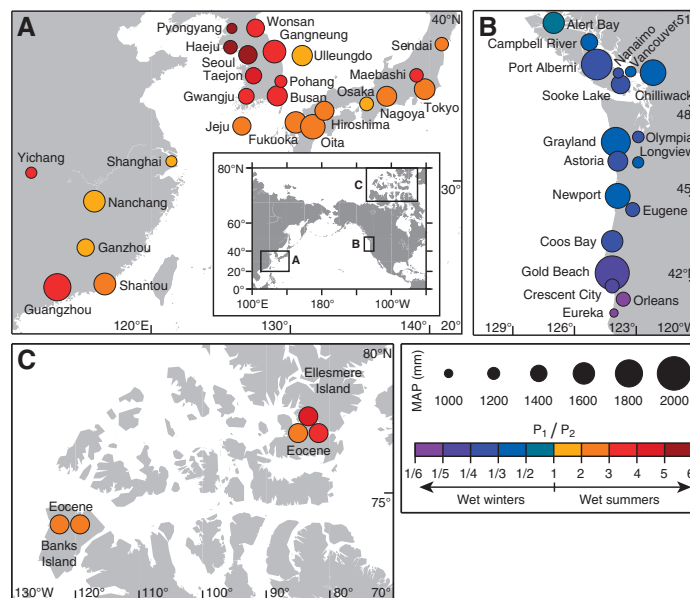
Figure 2. Comparison of mean annual precipitation (MAP) and seasonal precipitation (P_1—May through October; P_2—November through April). Precipitation data are presented for (A) modern eastern Asia, (B) modern Pacific Northwest, and (C) Eocene Arctic Canada (Ellesmere Island, Banks Island). Although all three regions have similar MAP, precipitation across eastern Asia (i.e., Japan, South Korea, and eastern China) falls mostly in summer, while precipitation in the Pacific Northwest falls mostly in winter. The mean annual and seasonal precipitation in Arctic Canada during the Eocene (C) is very similar to eastern Asia (A), and opposite in seasonality to the Pacific Northwest (B). Precipitation data are from Environment Canada (2011), NOAA Climate Services (2011), and Western Regional Climate Center (2011).

In conclusion, we envision that ecosystems across the Canadian Arctic during the Eocene were highly seasonal with respect to precipitation, and received ~76% of the total annual precipitation during the summer months of nearly continuous light.

REFERENCES CITED

Abbot, D.S., Huber, M., Bousquet, G., and Walker, C.C., 2009, High-CO_2 cloud radiative forcing feedback over both land and ocean in a global climate model: Geophysical Research Letters, v. 36, L05702, doi:10.1029/2008GL036703.

Barbour, M.M., Walcroft, A.S., and Farquhar, G.D., 2002, Seasonal variation in $\delta^{13}C$ and $\delta^{18}O$ of cellulose from growth rings of *Pinus radiata*: Plant, Cell & Environment, v. 25, p. 1483–1499, doi:10.1046/j.0016-8025.2002.00931.x.

Barke, J., Abels, H.A., Sangiorgi, F., Greenwood, D.R., Sweet, A.R., Donders, T., Reichart, G.-J., Lotter, A.F., and Brinkhuis, H., 2011, Orbitally forced *Azolla* blooms and Middle Eocene Arctic hydrology: Clues from palynology: Geology, v. 39, p. 427–430, doi:10.1130/G31640.1.

Basinger, J.F., 1991, The fossil forests of the Buchanan Lake Formation (early Tertiary), Axel Heiberg Island, Canadian Arctic archipelago: Preliminary floristics and paleoclimate, *in* Christie, R.L., and McMillan, N.J., eds., Tertiary fossil forests of the Geodetic Hills, Axel Heiberg Island, Arctic Archipelago: Geological Survey of Canada Bulletin 403, p. 39–65.

Basinger, J.F., Greenwood, D.R., and Sweda, T., 1994, Early Tertiary vegetation of Arctic Canada and its relevance to paleoclimatic interpretation, *in* Boulter, M.C., and Fisher, H.C., eds., Cenozoic plants and climates of the Arctic: Berlin, Springer-Verlag, p. 175–198.

Brinkhuis, H., Schouten, S., Collinson, M.E., Sluijs, A., Damsté, J.S.S., Dickens, G.R., Huber, M., Cronin, T.M., Onodera, J., Takahashi, K., Bujak, J.P., Stein, R., van der Burgh, J., Eldrett, J.S., Harding, I.C., Lotter, A.F., Sangiorgi, F., Cittert, H.V.V., de Leeuw, J.W., Matthiessen, J., Backman, J., and Moran, K., and the Expedition 302 Scientists, 2006, Episodic fresh surface waters in the Eocene Arctic Ocean: Nature, v. 441, p. 606–609, doi:10.1038/nature04692.

Eberle, J.J., and McKenna, M.C., 2002, Early Eocene Leptictida, Pantolesta, Creodonta, Carnivora, and Mesonychidae (Mammalia) from the Eureka Sound Group, Ellesmere Island, Nunavut: Canadian Journal of Earth Sciences, v. 39, p. 899–910, doi:10.1139/e02-001.

Eberle, J., Fricke, H., and Humphrey, J., 2009, Lower-latitude mammals as year-round residents in Eocene Arctic forests: Geology, v. 37, p. 499–502, doi:10.1130/G25633A.1.

Eberle, J.J., Fricke, H.C., Humphrey, J.D., Hackett, L., Newbrey, M.G., and Hutchison, J.H., 2010, Seasonal variability in Arctic temperatures during early Eocene time: Earth and Planetary Science Letters, v. 296, p. 481–486, doi:10.1016/j.epsl.2010.06.005.

Environment Canada, 2011, National Climate Data and Information Archive: http://climate.weatheroffice.gc.ca (December 2011).

Estes, R., and Hutchison, J.H., 1980, Eocene lower vertebrates from Ellesmere Island, Canadian Arctic Archipelago: Palaeogeography, Palaeoclimatology, Palaeoecology, v. 30, p. 325–347, doi:10.1016/0031-0182(80)90064-4.

GEOMAR, 2011, Ocean Drilling Stratigraphic Network Plate Tectonic Reconstruction Service: http://www.odsn.de/odsn/services/paleomap/paleomap.html (December 2011).

Greenwood, D.R., Basinger, J.F., and Smith, R.Y., 2010, How wet was the Arctic Eocene rain forest? Estimates of precipitation from Paleogene Arctic macrofloras: Geology, v. 38, p. 15–18, doi:10.1130/G30218.1.

Harrington, G.J., Eberle, J., LePage, B.A., Dawson, M., and Hutchison, J.H., 2011, Arctic plant diversity in the Early Eocene greenhouse: Proceedings of the Royal Society, ser. B, doi:10.1098/rspb.2011.1704.

Helle, G., and Schleser, G.H., 2004, Beyond CO_2-fixation by Rubisco—An interpretation of $^{13}C/^{12}C$ variations in tree rings from novel intra-seasonal studies on broad-leaf trees: Plant, Cell & Environment, v. 27, p. 367–380, doi:10.1111/j.0016-8025.2003.01159.x.

Herman, A.B., and Spicer, R.A., 2010, Mid-Cretaceous floras and climate of the Russian high Arctic (Novosibirsk Islands, Northern Yakutiya): Palaeogeography, Palaeoclimatology, Palaeoecology, v. 295, p. 409–422, doi:10.1016/j.palaeo.2010.02.034.

Irving, E., and Wynne, P.J., 1991, The paleolatitude of the Eocene fossil forests of Arctic Canada, *in* Christie, R.L., and McMillan, N.J., eds., Tertiary fossil forests of the Geodetic Hills, Axel Heiberg Island, Arctic Archipelago: Geological Survey of Canada Bulletin 403, p. 209–211.

Jahren, A.H., 2007, The Arctic forest of the middle Eocene: Annual Review of Earth and Planetary Sciences, v. 35, p. 509–540, doi:10.1146/annurev.earth.35.031306.140125.

Jahren, A.H., and Sternberg, L.S.L., 2003, Humidity estimate for the middle Eocene Arctic rain forest: Geology, v. 31, p. 463–466, doi:10.1130/0091-7613(2003)031<0463:HEFTME>2.0.CO;2.

Jahren, A.H., and Sternberg, L.S.L., 2008, Annual patterns within tree rings of the Arctic middle Eocene (ca. 45 Ma): Isotopic signatures of precipitation, relative humidity, and deciduousness: Geology, v. 36, p. 99–102, doi:10.1130/G23876A.1.

Kalgutkar, R.M., and McIntyre, D.J., 1991, Helicosporous fungi and Early Eocene pollen, Eureka Sound Group, Axel Heiberg Island, Northwest Territories: Canadian Journal of Earth Sciences, v. 28, p. 364–371, doi:10.1139/e91-033.

Keeling, C.D., Piper, S.C., Bacastow, R.B., Wahlen, M., Whorf, T.P., Heimann, M., and Meijer, H.A., 2001, Exchanges of atmospheric CO_2 and $^{13}CO_2$ with the terrestrial biosphere and oceans from 1978 to 2000. I. Global aspects: San Diego, Scripps Institution of Oceanography, SIO Reference Series, 88 p.

Korea Meteorological Administration, 2011, 30-year average climate data: http://www.kma.go.kr/weather/climate/average_30years.jsp?yy_st=2011&stn=159&norm=M&x=33&y=16&obs=0&mm=5&dd=27 (January 28–February 25, 2011).

Leavitt, S.W., and Long, A., 1991, Seasonal stable-carbon isotope variability in tree rings: Possible paleoenvironmental signals: Chemical Geology (Isotope Geoscience Section), v. 87, p. 59–70.

Markwick, P.J., 1998, Fossil crocodilians as indicators of Late Cretaceous and Cenozoic climates: Implications for using palaeontological data in reconstructing palaeoclimate: Palaeogeography, Palaeoclimatology, Palaeoecology, v. 137, p. 205–271, doi:10.1016/S0031-0182(97)00108-9.

McIntyre, D.J., 1991, Pollen and spore flora of an Eocene forest, eastern Axel Heiberg Island, N.W.T., *in* Christie, R.L., and McMillan, N.J., eds., Tertiary fossil forests of the Geodetic Hills, Axel Heiberg Island, Arctic Archipelago: Geological Survey of Canada Bulletin 403, p. 83–97.

McIver, E.E., and Basinger, J.F., 1999, Early Tertiary floral evolution in the Canadian High Arctic: Annals of the Missouri Botanical Garden, v. 86, p. 523–545, doi:10.2307/2666184.

NOAA Climate Services, 2011, Monthly surface data: http://gis.ncdc.noaa.gov/map/monthly (December 2011).

Pons, T.L., and Helle, G., 2011, Identification of anatomically non-distinct annual rings in tropical trees using stable isotopes: Trees—Structure and Function, v. 25, p. 83–93, doi:10.1007/s00468-010-0527-5.

Schubert, B.A., and Jahren, A.H., 2011, Quantifying seasonal precipitation using high-resolution carbon isotope analyses in evergreen wood: Geochimica et Cosmochimica Acta, v. 75, p. 7291–7303, doi:10.1016/j.gca.2011.08.002.

Western Regional Climate Center, 2011, Western U.S. Climate Historical Summaries: Period of record monthly climate summary: http://www.wrcc.dri.edu/climsum.html (January 28–February 25, 2011).

Williams, C.J., Johnson, A.H., LePage, B.A., Vann, D.R., and Sweda, T., 2003, Reconstruction of Tertiary *Metasequoia* forests. II. Structure, biomass, and productivity of Eocene floodplain forests in the Canadian Arctic: Paleobiology, v. 29, p. 271–292, doi:10.1666/0094-8373(2003)029<0271:ROTMFI>2.0.CO;2.

Printed in USA

GSA DATA REPOSITORY 2012152

A summertime rainy season in the Arctic forests of the Eocene

Brian A. Schubert, A. Hope Jahren, Jaelyn J. Eberle, Leonel S.L. Sternberg, and David A. Eberth
correspondence to: bschube@hawaii.edu

Quantifying the Ratio of Summer to Winter Precipitation

Schubert and Jahren (2011) used high-resolution, intra-ring $\delta^{13}C$ data from angiosperm and gymnosperm evergreen species growing under different climates worldwide to relate average seasonal changes in environmental parameters to average seasonal changes in the $\delta^{13}C$ value ($\Delta\delta^{13}C$) using the following general equation:

$$\Delta\delta^{13}C = \Delta\delta^{13}C_{CO2} + A(\Delta P) + B(\Delta T) + C(d) + D(\Delta c_a) + \Delta Y \quad (1)$$

where $\Delta\delta^{13}C_{CO2}$, ΔP, ΔT, and Δc_a are the average, seasonal changes in $\delta^{13}C_{CO2}$, precipitation, temperature, and carbon dioxide concentration, respectively. *A*, *B*, *C*, and *D* are constant scalars, *d* is the distance in degrees latitude from the equator (a proxy for changes in seasonal light levels), and ΔY represents seasonal changes post-photosynthetic physiological processes. Seasonal changes in precipitation and temperature were defined as follows:

$$\Delta P = \ln(P_1) - \ln(P_2) \quad (2)$$
$$\Delta T = \ln(T_1) - \ln(T_2) \quad (3)$$

where subscripts 1 and 2 indicate the 6-month period (May through October or November through April) during which the maximum and minimum $\delta^{13}C$ values occur, respectively. For northern hemisphere sites, $\Delta\delta^{13}C_{CO2}$ can be calculated using data from Keeling et al. (2001) such that:

$$\Delta\delta^{13}C_{CO2} = 0.01(L) + 0.13 \quad (4)$$

where *L* is latitude. Optimization of Equation 1 showed that $\Delta\delta^{13}C$ varied among sites based on seasonal changes in $\delta^{13}C_{CO2}$ and precipitation (i.e., $A = -0.82$, $B = 0$, $C = 0$, $D = 0$):

$$\Delta\delta^{13}C = \Delta\delta^{13}C_{CO2} - 0.82(\Delta P) + 0.73 \quad \text{(5; same as Equation 9 within Schubert and Jahren, 2011).}$$

Substituting Equation 2 into Equation 5 and rearranging to solve for $\ln(P_1/P_2)$ yields:

$$\ln(P_1/P_2) = (\Delta\delta^{13}C_{meas} - \Delta\delta^{13}C_{CO2} - 0.73) / -0.82 \quad \text{(6; same as Equation 1 of the main text).}$$

Substitution of Equation 4 into Equation 6 provides and equation for calculating P_1/P_2 from $\Delta\delta^{13}C$ and knowing latitude:

$$\ln(P_1/P_2) = (\Delta\delta^{13}C - 0.01(L) - 0.86) / -0.82 \quad (7).$$

Stable Carbon Isotope Analysis

Bulk $\delta^{13}C$ values were measured via online combustion using a Eurovector automated elemental analyzer (Eurovector Inc, Milan, Italy) coupled to an Isoprime isotope ratio mass spectrometer (Isoprime, Ltd, Cheadle Hulme, UK); all samples were introduced to the combustion system in pure tin capsules. Our choice to measure $\delta^{13}C$ in bulk wood is consistent with several published examples that prefer bulk wood in order to expedite high-resolution sampling (Schulze et al., 2004) and reduce bias (Walia et al., 2010). All isotope data used to develop our seasonal precipitation model (Schubert and Jahren, 2011) represent $\delta^{13}C$ determinations in bulk wood, except for one study that reported holocellulose, one on α-cellulose, and one that measured both bulk wood and cellulose. Multiple studies have demonstrated that there is a consistent isotopic offset between bulk wood and cellulose fractions and therefore a similar intra-ring $\delta^{13}C$ pattern (Leavitt and Long, 1991; Pons and Helle, 2011; Verheyden et al., 2005), including for fossil wood (compare Fig 2B and 2C within Jahren and Sternberg, 2008). Isotopic values are reported in δ-notation (‰) against Vienna standards (VPDB). Analytical uncertainty associated with each measurement was <0.1 ‰. Each $\delta^{13}C$ value determined from samples G13, A15A16, and MB represents the average of three replicate capsules; the average isotopic variability of replicate capsules was ± 0.08‰. Each $\delta^{13}C$ value determined from samples CMNPB4720 and CMNPB4723 represents a single measurement.

Age of the Stenkul Fiord Wood Samples

We estimate the age of the fossil wood samples from the Margaret Formation at Stenkul Fiord, southern Ellesmere Island, Nunavut based primarily upon the composition of the vertebrate fauna that includes mammals and several taxa of turtle, and to a lesser extent the palynology and a preliminary radiometric date. The terrestrial fossil-bearing sediments of the Margaret Formation comprise inter-bedded sandstone, mudstone, and coal that are interpreted to represent a lush proximal delta front to delta plain environment with abundant channels and coal swamps (Miall, 1986).

Sample MB was collected from a sandy unit (Fig. DR2) in western exposures of the Margaret Formation (Eureka Sound Group) along the southern shore of Stenkul Fiord (77 °N) that also produced fossils of the hippo-like *Coryphodon*, perissodactyls (including tapiroids), and the turtle taxa *Echmatemys*, *Hadrianus*, and Emydidae (pond turtles). The vertebrate taxa suggest an age of Early Eocene (Wasatchian North American Land Mammal 'Age') that is corroborated by pollen floras (Harrington et al., 2011). As additional age control, a zircon recovered from volcanic ash located at the base of the

stratigraphic sections on the southern shore of Stenkul Fiord yielded preliminary dates by SHRIMP analysis of 52.6 ± 1.9 Ma (Reinhardt et al., 2010).

The other two samples – G13 and A15A16 – were recovered from exposures of the Eureka Sound Group along the eastern shore of Stenkul Fiord (Fig. DR3). Although vertebrate fossils are rare in this section, there is some evidence for an early Eocene age. Specifically, a fossil of a perissodactyl was recovered from approximately the same stratigraphic level as A15A16. Perissodactyls first appeared in North America at the onset of the Eocene (Bowen et al., 2002). However, wood sample G13 comes from a stratigraphic level that is below this and consequently its age may be early Eocene or potentially latest Paleocene. Fossils of trionychine (soft-shelled) turtle and the alligator *Allognathosuchus* occur throughout the section at Stenkul Fiord, but are not temporally diagnostic.

Muskox River Age Model

The wood samples from the Muskox River site on northern Banks Island, Northwest Territories (~74˚N) were collected from the Cyclic Member of the Eureka Sound Formation. The Cyclic Member comprises coarsening-upward cycles of shale, silt, unconsolidated sand, paleosol, and lignitic coal, interpreted as a deltaic sequence (Miall, 1979) (Fig. DR4), and the trees probably grew on delta lobes. On the basis of palynology, the Muskox River site is Eocene in age, and probably Early Eocene. Specifically, the presence of *Platycarya* [reported by Hopkins (1974) in Miall (1979)] in a pollen sample collected from GSC loc. C-26412 at the Muskox River site suggests an Early Eocene age, although this occurrence needs to be verified through analysis of new pollen samples (collected in 2010) that are underway (A.R. Sweet, pers. comm., 2011). Although of limited biostratigraphic utility, the fossil vertebrates known from northern Banks Island support the pollen-based Eocene age estimate. Specifically, rare fossil turtle shell fragments collected by JJE in 2004 at nearby Eames River (north of the Muskox River site, and mapped by (Miall, 1979) as Eocene in age) and identified by J.H. Hutchison (UCMP Berkeley) are referred to Emydidae (pond turtles), a family that appeared in mid-latitude North America in the early Wasatchian [Wa1; (Holroyd et al., 2001; Hutchison, 1998)]. Further, isolated sharks' teeth referred to the genus *Physogaleus* (Carcharhinidae; extinct relative of today's sharpnose sharks) are known from the Muskox River site (Padilla, 2008), a genus documented only from Eocene-aged strata elsewhere (Cappetta, 1987; Rana et al., 2006; Takeshi et al., 2006), while thousands of sharks' teeth referred to *Striatolamia* (Odontaspididae; sand tigers) are known from both the Muskox River and Eames River sites, and this genus has a Paleocene-Eocene distribution (Padilla, 2008).

Significance of Evergreen Wood

Although deciduous flora dominated Arctic environments during parts of the Eocene (Jahren, 2007; Jahren and Sternberg, 2008), evergreen cones and leaves (Kotyk et al., 2003) and pollen (e.g., Harrington et al., 2011) have been identified. Our samples,

however, mark the first examples of evergreen wood from the Eocene Arctic. Earlier studies claimed to have identified *Picea* wood (evergreen), however, reanalysis of the wood indicated the samples were actually *Larix* (deciduous) (Jagels et al., 2001). The presence of evergreen wood, although relatively rare, should not be surprising given the observations made by Royer et al. (2003, 2005) that from a carbon loss perspective, under extreme photoperiod deciduous strategies do not confer an advantage over evergreens. In addition, evergreen foliage may have provided a winter food source for large, non-migratory mammals (Eberle et al., 2009).
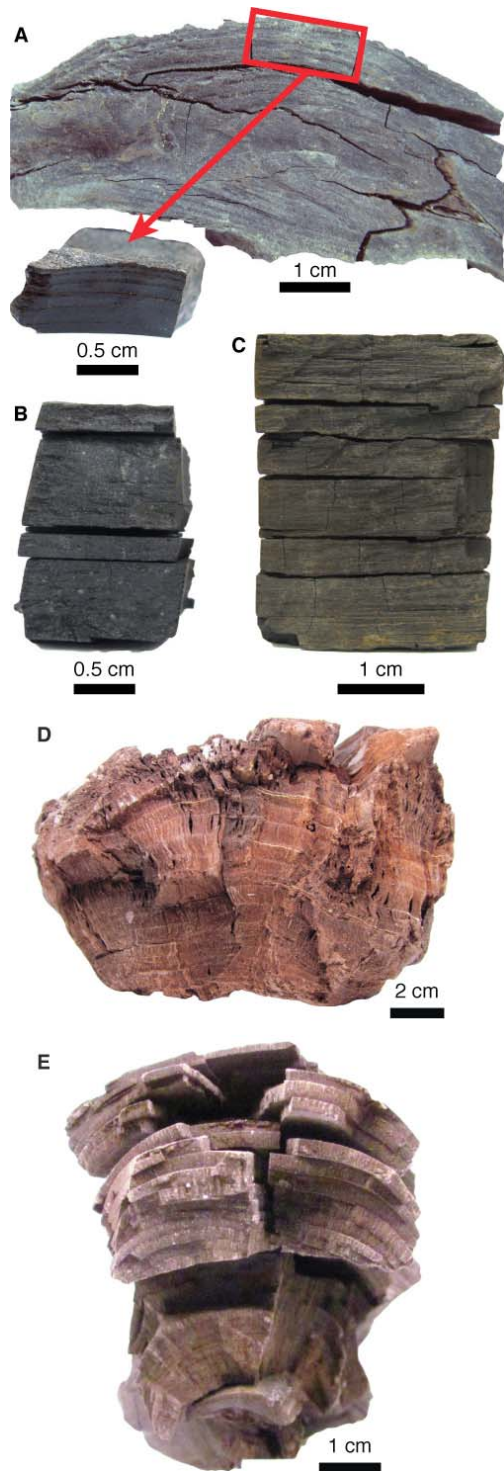
Figure DR1. Non-permineralized, evergreen fossil-wood from Ellesmere Island (A-C) and Banks Island (D-E). (A) MB, a concentric sample, contained visible tree rings. Inset shows subsample used for high-resolution δ^{13}C analysis. (B) G13 and (C) A15A16 both lacked preserved ring anatomy. (D) CMNPB4720 and (E) CMNPB4723 are both concentric, ringed samples. Note that fractures, caused by shrinkage upon drying, do not necessarily follow ring contours and do not indicate ring boundaries.
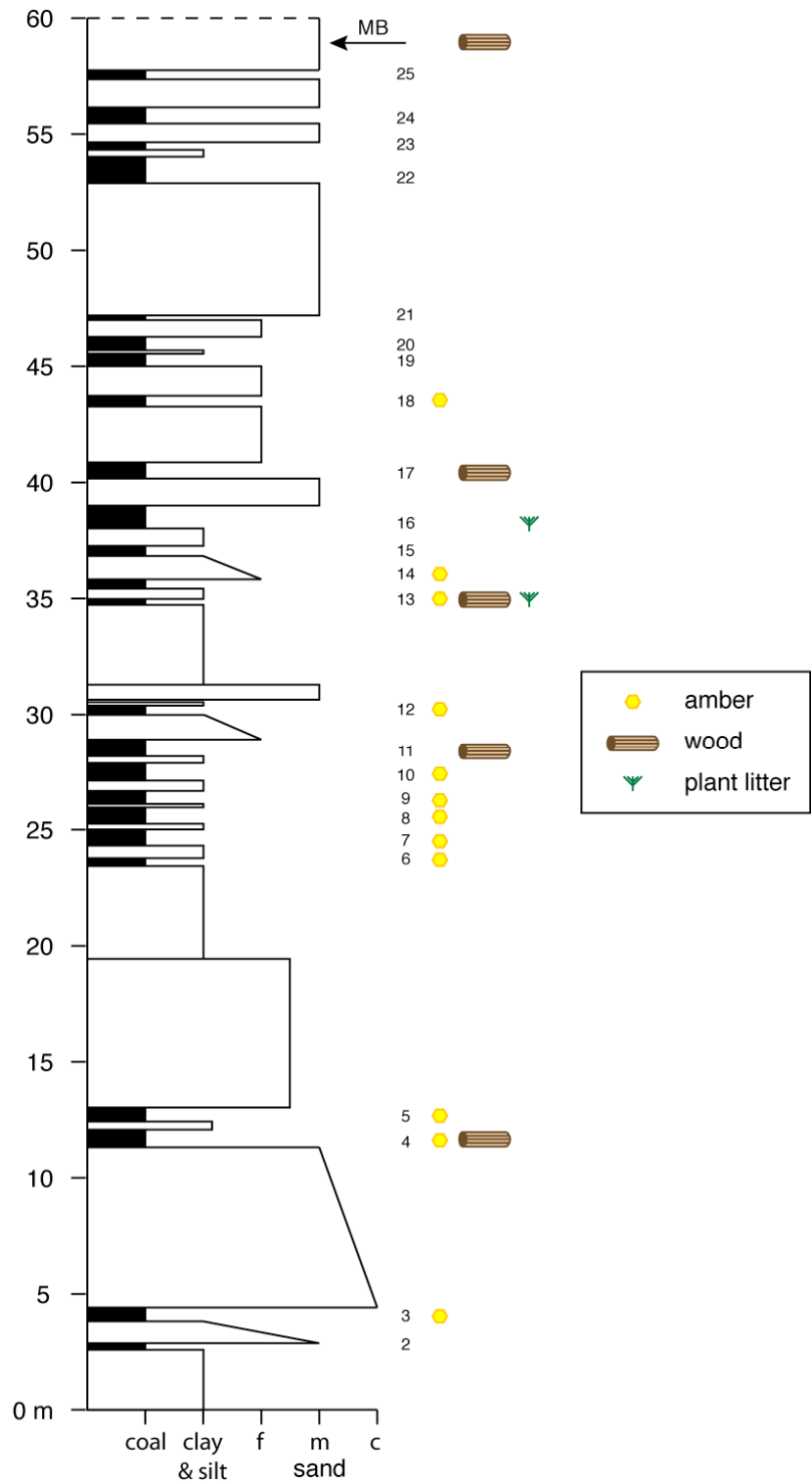
Figure DR2. Stratigraphic sequence of the western exposure of the Margaret Formation (Eureka Sound Group) along the southern shore of Stenkul Fiord. The location of sample MB is indicated. This sequence corresponds in part to CR-83-14 described in Kalkreuth et al. (1996). Coal layers are numbered sequentially from bottom to top.
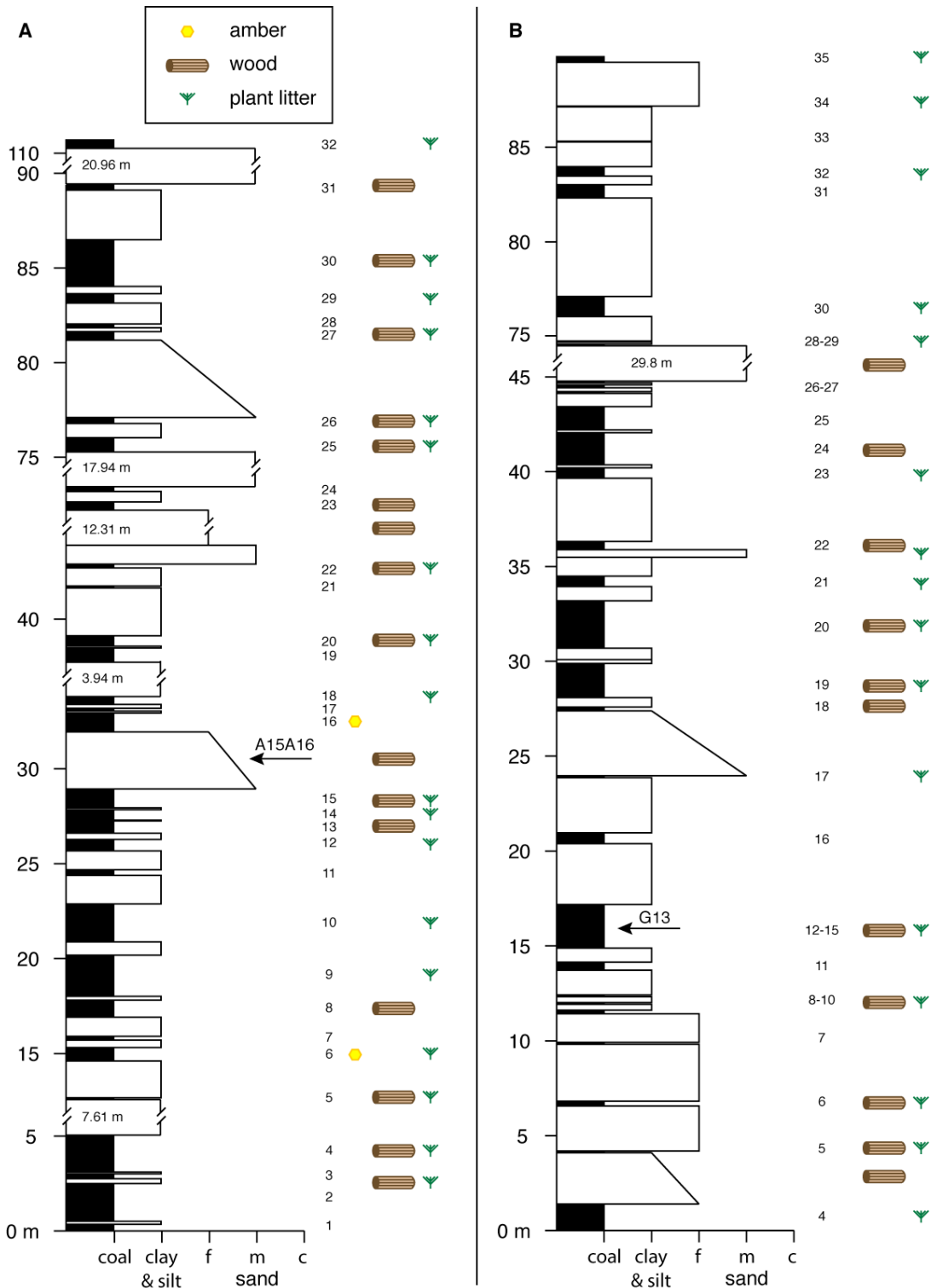
Figure DR3. Stratigraphic sequences of exposures of the Eureka Sound Group along the eastern shore of Stenkul Fiord from which samples A15A16 (A) and G13 (B) were recovered. (A) Section corresponds in part to CR-83-07 (Kalkreuth et al., 1996). (B) Section corresponds in part to CR-83-10 (Kalkreuth et al., 1996). Coal layers in both are numbered sequentially from bottom to top.
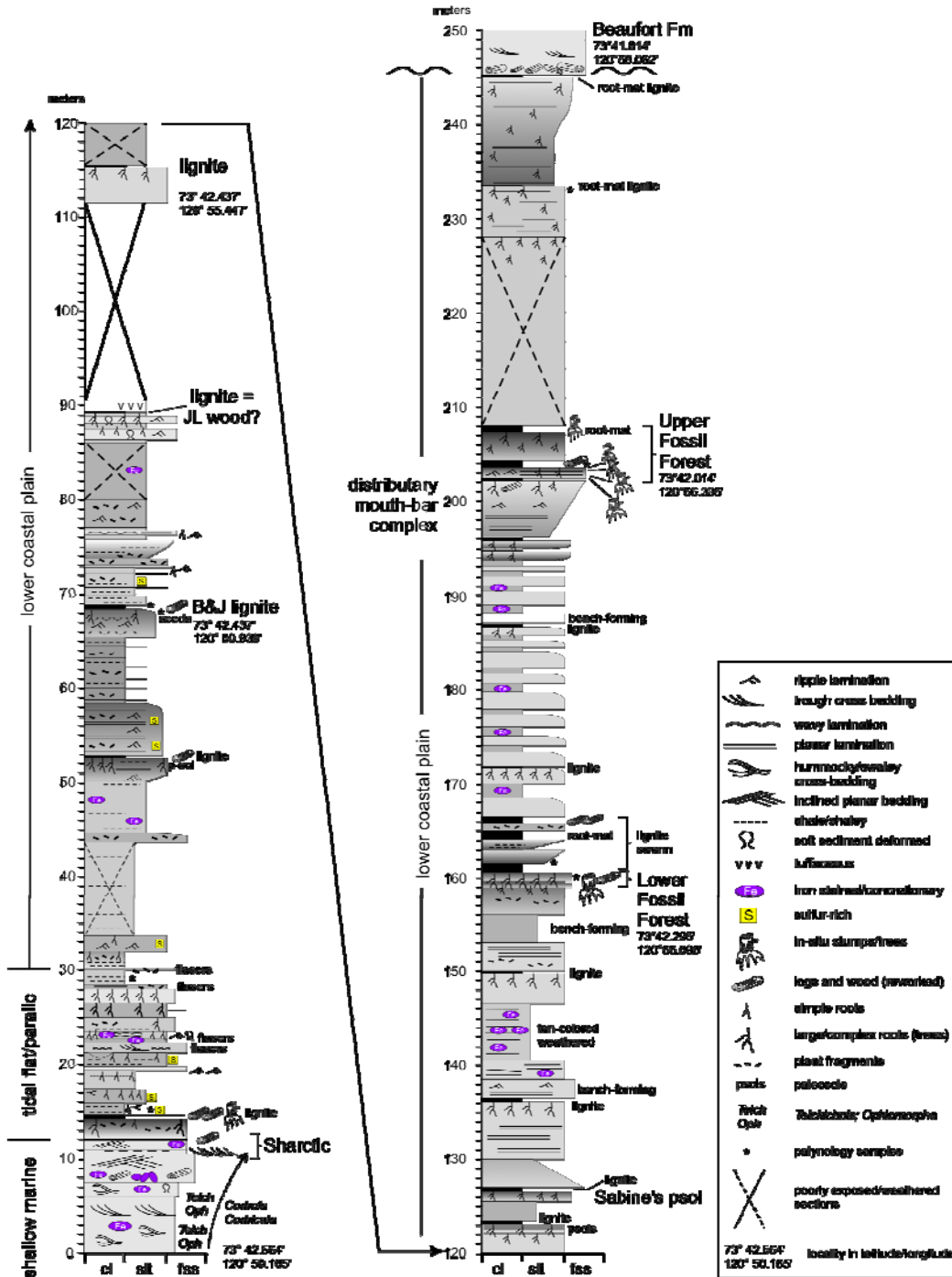
Figure DR4. Composite measured section through the exposures of the Eureka Sound Formation at Muskox River, north-central Banks Island. Section transect is indicated by latitude and longitude coordinates at various highlighted localities. Overall, the section records deposition in a lower coastal plain setting characterized by distributary mouth-bar complexes and extensive wetlands (Miall, 1979). Samples CMNPB4720 and CMNPB4723 were collected from the "Upper Fossil Forest" layers.

REFERENCES CITED

Bowen, G. J., Clyde, W. C., Koch, P. L., Ting, S., Alroy, J., Tsubamoto, T., Wang, Y., and Wang, Y., 2002, Mammalian dispersal at the Paleocene/Eocene Boundary: Science, v. 295, no. 5562, p. 2062-2065.

Cappetta, H., 1987, Chondrichthyes II: Mesozoic and Cenozoic Elasmobranchii, Stuttgart, Gustav Fischer Verlag, Handbook of Paleoichthyology, Volume 3B, 193 p.:

Eberle, J., Fricke, H., and Humphrey, J., 2009, Lower-latitude mammals as year-round residents in Eocene Arctic forests: Geology, v. 37, no. 6, p. 499-502.

Harrington, G. J., Eberle, J., LePage, B. A., Dawson, M., and Hutchison, J. H., 2011, Arctic plant diversity in the Early Eocene greenhouse: Proceedings of the Royal Society B.

Holroyd, P. A., Hutchison, J. H., and Strait, S. G., 2001, Turtle diversity and abundance through the lower Eocene Willwood Formation of the southern Bighorn Basin: University of Michigan Papers on Paleontology, v. No. 33, p. 97-107.

Hopkins, W. S., 1974, Report on 36 Field Samples from Banks Island, District of Franklin, Northwest Territories, Submitted by A. Miall, 1973 (NTS 88C, F, 98D, E): Geological Survey of Canada, Paleontological Report KT-01-WSH-1974, p. 1-12.

Hutchison, J. H., 1998, Turtles across the Paleocene/Eocene Epoch boundary in west-central North America, *in* Aubry, M.-P., Lucas, S., and Berggren, W. A., eds., Late Paleocene–Early Eocene Climate and Biotic Events in the Marine and Terrestrial Records: New York, Columbia Univ. Press, p. 401-408.

Jagels, R., LePage, B. A., and Jiang, M., 2001, Definitive identification of *Larix* (Pinaceae) wood based on anatomy from the Middle Eocene, Axel Heiberg Island, Canadian High Arctic: IAWA Journal, v. 22, no. 1, p. 73-83.

Jahren, A. H., 2007, The Arctic forest of the middle Eocene: Annual Review of Earth and Planetary Sciences, v. 35, p. 509-540.

Jahren, A. H., and Sternberg, L. S. L., 2008, Annual patterns within tree rings of the Arctic middle Eocene (ca. 45 Ma): Isotopic signatures of precipitation, relative humidity, and deciduousness: Geology, v. 36, no. 2, p. 99-102.

Kalkreuth, W. D., Riediger, C. L., McIntyre, D. J., Richardson, R. J. H., Fowler, M. G., and Marchioni, D., 1996, Petrological, palynological and geochemical characteristics of Eureka Sound Group coals (Stenkul Fiord, southern Ellesmere Island, Arctic Canada): International Journal of Coal Geology, v. 30, p. 151-182.

Keeling, C. D., Piper, S. C., Bacastow, R. B., Wahlen, M., Whorf, T. P., Heimann, M., and Meijer, H. A., 2001, Exchanges of atmospheric CO_2 and $^{13}CO_2$ with the terrestrial biosphere and oceans from 1978 to 2000. I. Global aspects, San Diego, Scripps Institution of Oceanography, SIO Reference Series, 88 p.:

Kotyk, M. E. A., Basinger, J. F., and McIver, E. E., 2003, Early Tertiary *Chamaecyparis* Spach from Axel Heiberg Island, Canadian High Arctic: Canadian Journal of Botany, v. 81, no. 2, p. 113-130.

Leavitt, S. W., and Long, A., 1991, Seasonal stable-carbon isotope variability in tree rings: possible paleoenvironmental signals: Chemical Geology (Isotope Geoscience Section), v. 87, p. 59-70.

Miall, A. D., 1979, Mesozoic and Tertiary geology of Banks Island, Arctic Canada: Geological Survey of Canada Memoir, v. 387, p. 1-235.

Miall, A. D., 1986, The Eureka Sound Group (Upper Cretaceous - Oligocene), Canadian Arctic Islands: Bulletin of Canadian Petroleum Geology, v. 34, p. 240-270.

Padilla, A., 2008, Faunal description and paleobiology of Eocene sharks from Banks Island in the Canadian Arctic: University of Colorado Masters Thesis, p. pp. 57.

Pons, T. L., and Helle, G., 2011, Identification of anatomically non-distinct annual rings in tropical trees using stable isotopes: Trees-Structure and Function, v. 25, no. 1, p. 83-93.

Rana, R. S., Kumar, K., Loyal, R. S., Sahni, A., Rose, K. D., Mussell, J., Singh, H., and Kulshreshtha, S. K., 2006, Selachians from the early Eocene Kapurdi Formation (Fuller's earth), Barmer District, Rajasthan: Journal of the Geological Society of India, v. 67, p. 509-522.

Reinhardt, L., Andruleit, H., Estrada, S., Henjes-Kunst, F., Piepjohn, K., von Gosen, W., Davis, D. W., and Davis, B., 2010, Altered volcanic ashes in Paleocene/Eocene Eureka Sound Group sediments (Ellesmere Island, Arctic Canada) – new stratigraphic tie-points?, GeoCanada: Calgary, Alberta.

Royer, D. L., Osborne, C. P., and Beerling, D. J., 2003, Carbon loss by deciduous trees in a CO2-rich ancient polar environment: Nature, v. 424, no. 6944, p. 60-62.

-, 2005, Contrasting seasonal patterns of carbon gain in evergreen and deciduous trees of ancient polar forests: Paleobiology, v. 31, no. 1, p. 141-150.

Schubert, B. A., and Jahren, A. H., 2011, Quantifying seasonal precipitation using high-resolution carbon isotope analyses in evergreen wood: Geochimica et Cosmochimica Acta, v. 75, no. 22, p. 7291-7303.

Schulze, B., Wirth, C., Linke, P., Brand, W. A., Kuhlmann, I., Horna, V., and Schulze, E. D., 2004, Laser ablation-combustion-GC-IRMS - a new method for online analysis of intra-annual variation of δ^{13}C in tree rings: Tree Physiology, v. 24, no. 11, p. 1193-1201.

Takeshi, T., Yoshitoma, F., and Satoshi, M., 2006, Fossil shark teeth from the Namigata Formation in Ibara City, Okayama Prefecture, central Japan and their biostratigraphical significance: Bulletin of the Mizunami Fossil Museum, v. 33, p. 103-109.

Verheyden, A., Roggeman, M., Bouillon, S., Elskens, M., Beeckman, H., and Koedam, N., 2005, Comparison between δ^{13}C of α-cellulose and bulk wood in the mangrove tree *Rhizophora mucronata*: Implications for dendrochemistry: Chemical Geology, v. 219, no. 1-4, p. 275-282.

Walia, A., Guy, R. D., and White, B., 2010, Carbon isotope discrimination in western hemlock and its relationship to mineral nutrition and growth: Tree Physiology, v. 30, no. 6, p. 728-740.